Electronic Supplementary Information

Biocompatible Hole Scavenger–Assisted Graphene Oxide Dots for Photodynamic Cancer Therapy

Chun-Yan Shih,[a] Wei-Lun Huang,[b] I-Ting Chiang,[b] Wu-Chou Su,[b,c] and Hsisheng Teng*[a, b, d]*

[a]Department of Chemical Engineering, National Cheng Kung University, Tainan 70101, Taiwan

[b]Center of Applied Nanomedicine, National Cheng Kung University, Tainan 70101, Taiwan

[c]Department of Internal Medicine, College of Medicine and Hospital, National Cheng Kung University, Tainan 70101, Taiwan

[d]Hierarchical Green-Energy Materials (Hi-GEM) Research Center, National Cheng Kung University, Tainan 70101, Taiwan

*Email: hteng@mail.ncku.edu.tw

*Email: sunnysu@mail.ncku.edu.tw

Table of Contents

8. Viability of the cancer and normal cells in H_2O_2

9. Population of viable cells in AnnV/PI-assay analysis

10. EPR for $^1O_2$ generation analysis

11. EPR for O_2^{-}•, HO_2•, and OH• generation analysis

12. Amplex® Red method for H_2O_2 quantification

1. Topographic analysis of NGODs

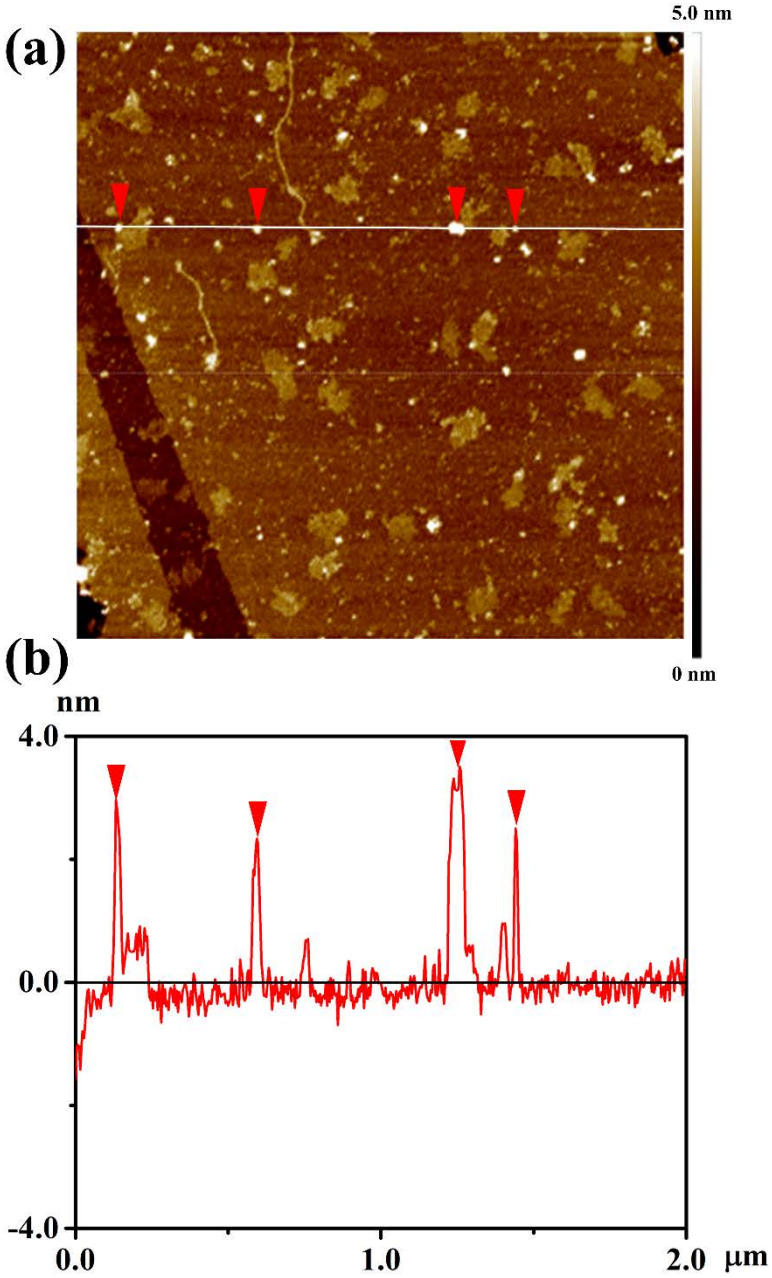

Fig. S1 (a) AFM image of the NGODs distributed on a mica substrate. (b) Height profile along the line in panel a

2. Full-range XPS spectrum of NGODs

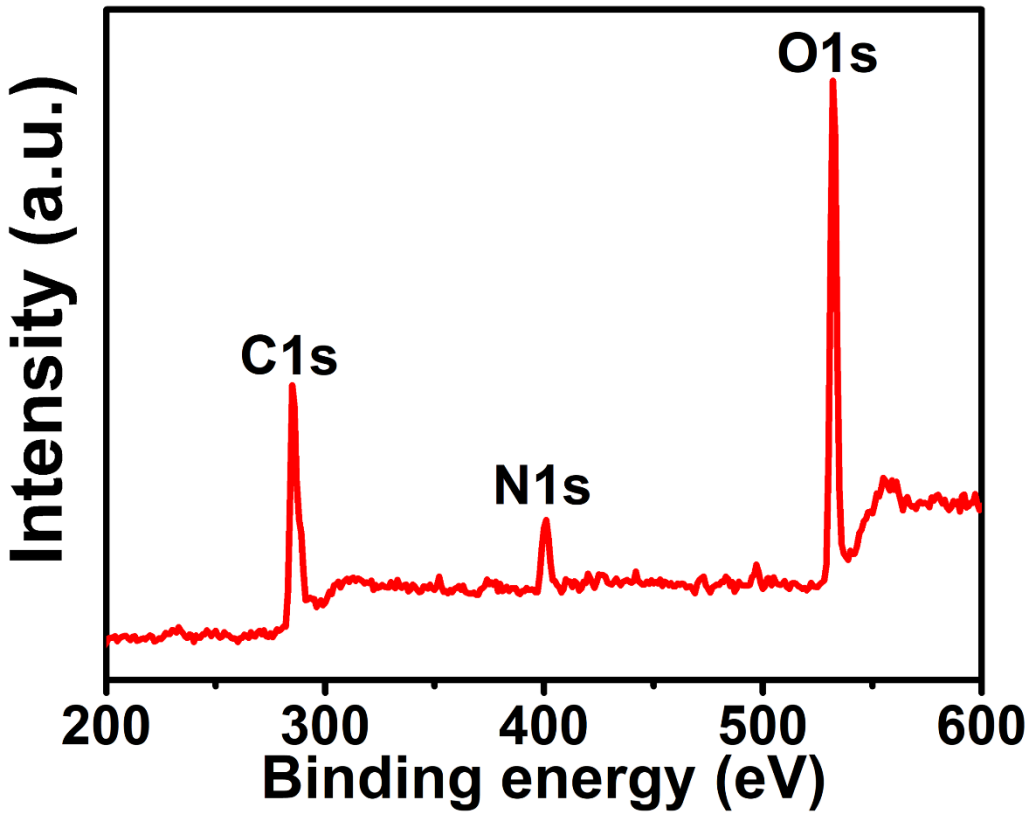

Fig. S2 Full-range XPS spectrum of NGODs.

3. Chemical composition of NGODs

Table S1 Atomic ratios of (N 1s)/(C 1s) and (O 1s)/(C 1s) determined from the full-range XPS spectra (Fig. S2), nitrogen functionality composition determined from the N 1s XPS spectrum (Fig. 1c), and carbon bonding composition determined from the C 1s XPS spectrum (Fig. 1d) for NGODs.

Atomic ratio (%)	Nitrogen functionality composition (% of C1s)				
N 1s / C 1s	Pyridine	Amino	Pyrrolic	Quaternary	Amide
16	0.47	1.9	4.4	4.7	4.4
Atomic ratio (%)	Carbon bonding composition (%)				
O 1s / C 1s	C–C	C–N	C–O	C=O	O–C=O
58	56	13	5.5	21	5.5

4. FTIR spectrum of NGODs

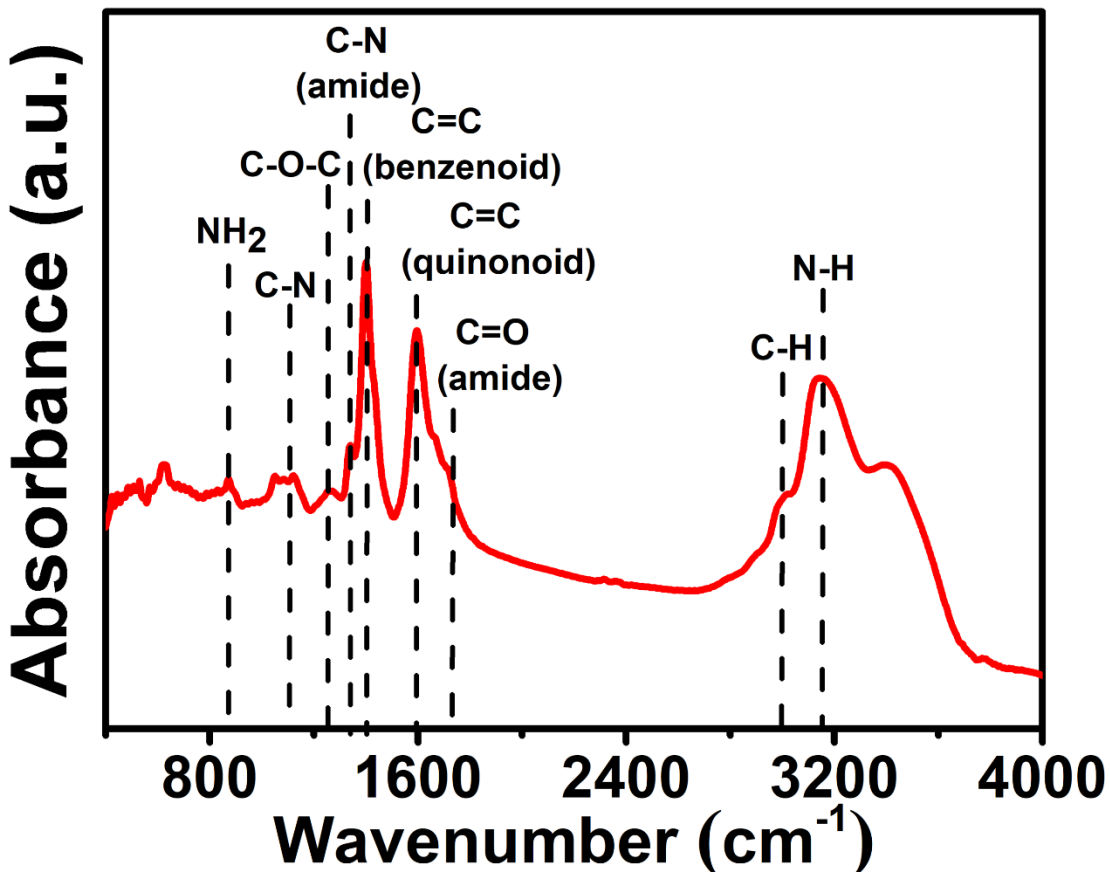

Fig. S3 FTIR absorption spectrum of NGODs.

5. UPS spectrum of NGODs

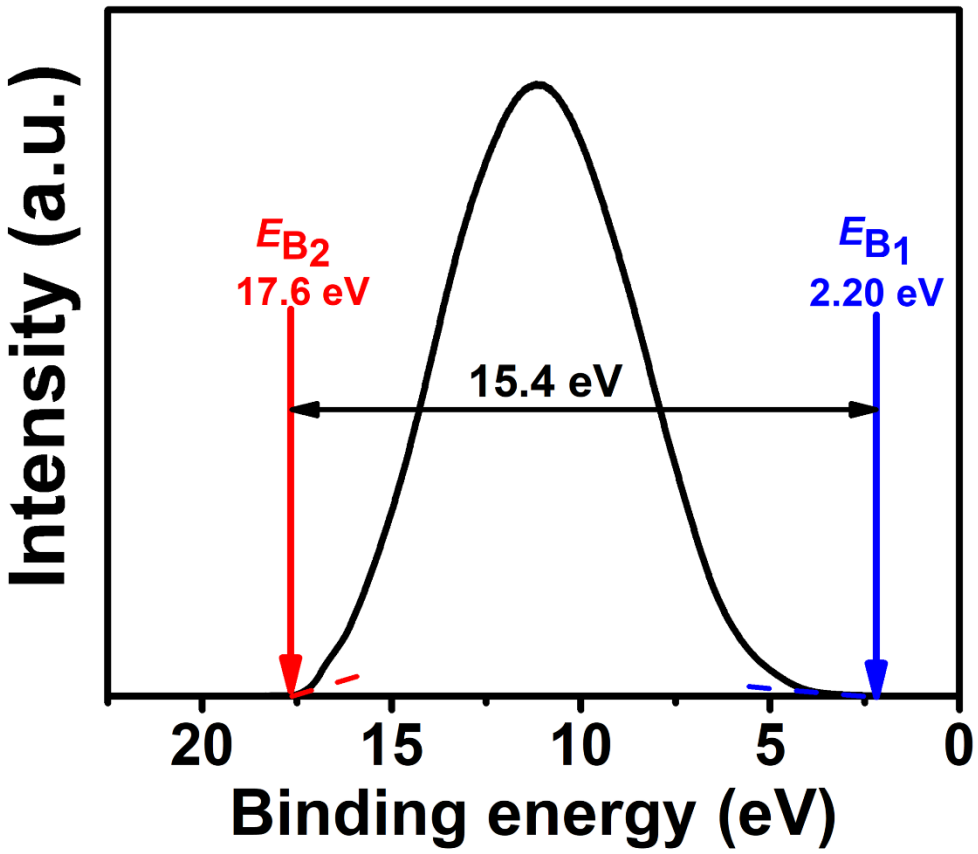

Fig. S4 UPS spectrum of NGODs. The electron onset binding energy values, E_{B1} and E_{B2}, were determined from the intercepts of the extrapolated tangent lines on the abscissa at low and high binding energies, respectively. The UPS width constituted the difference between E_{B1} and E_{B2}. The spectrum was obtained under He I light irradiation at 21.2 eV.

6. Spectrum of PDT light source

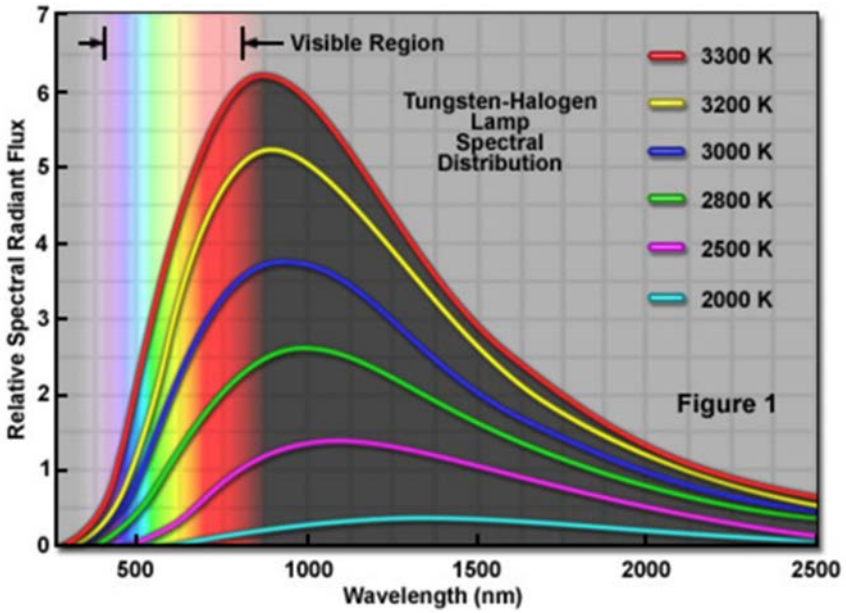

Fig. S5 Spectrum of tungsten–halogen incandescent light, obtained from the Carl Zeiss Microscopy Online C ampus website (http://zeiss-campus.magnet.fsu.edu/articles/lightsources/tungstenhalogen.html).

7. H_2O_2 generation from GO and NGOD suspensions

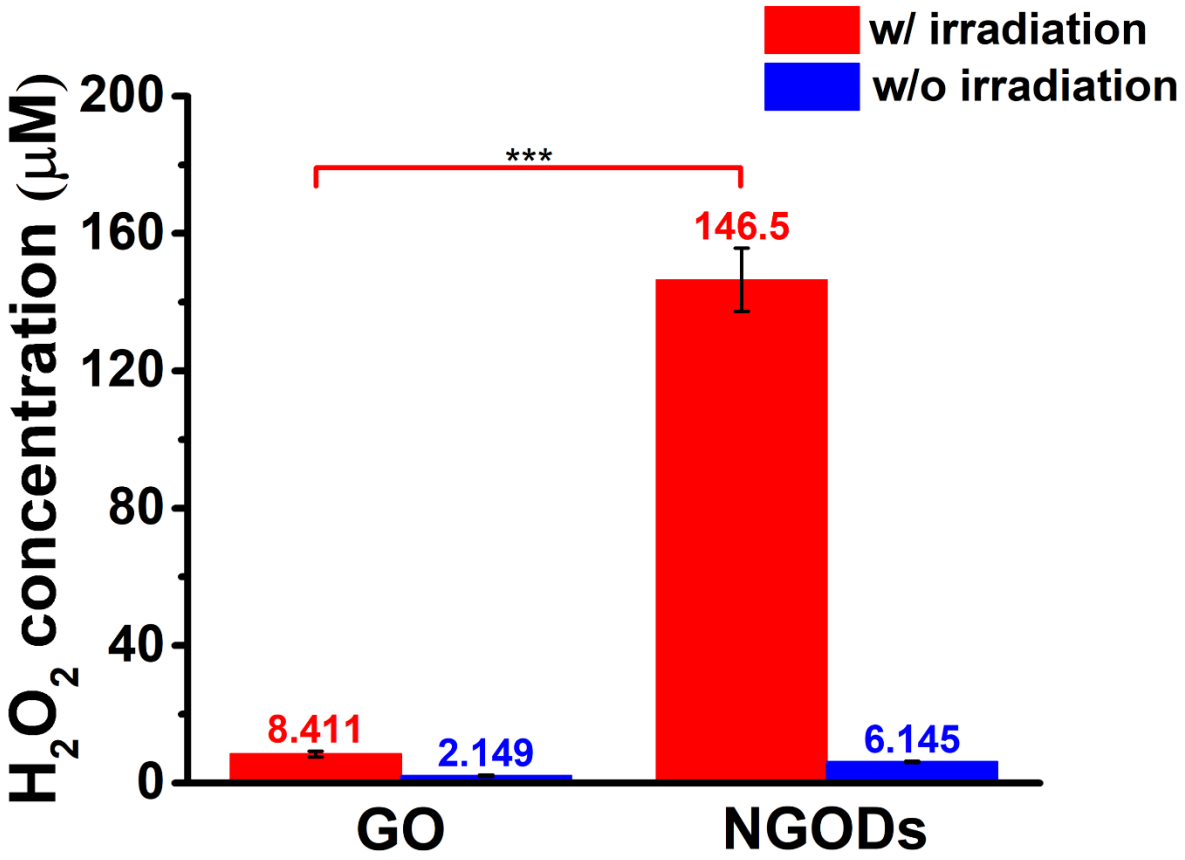

Fig. S6. H_2O_2 generation from the GO and NGOD suspensions containing 0.2 mM AA and 10 μg mL^{-1} of the GO or NGODs. The irradiation was conducted using the tungsten–halogen incandescent light at 40 mW cm^{-2} for 10 min. The plot presents the mean value of the data, whereas the error bars on each plot represent the standard error of the mean. The P values are indicated as *, **, and *** for $P < 0.05$, $P < 0.01$ and $P < 0.001$, respectively.

8. Viability of the cancer and normal cells under H_2O_2 treatment

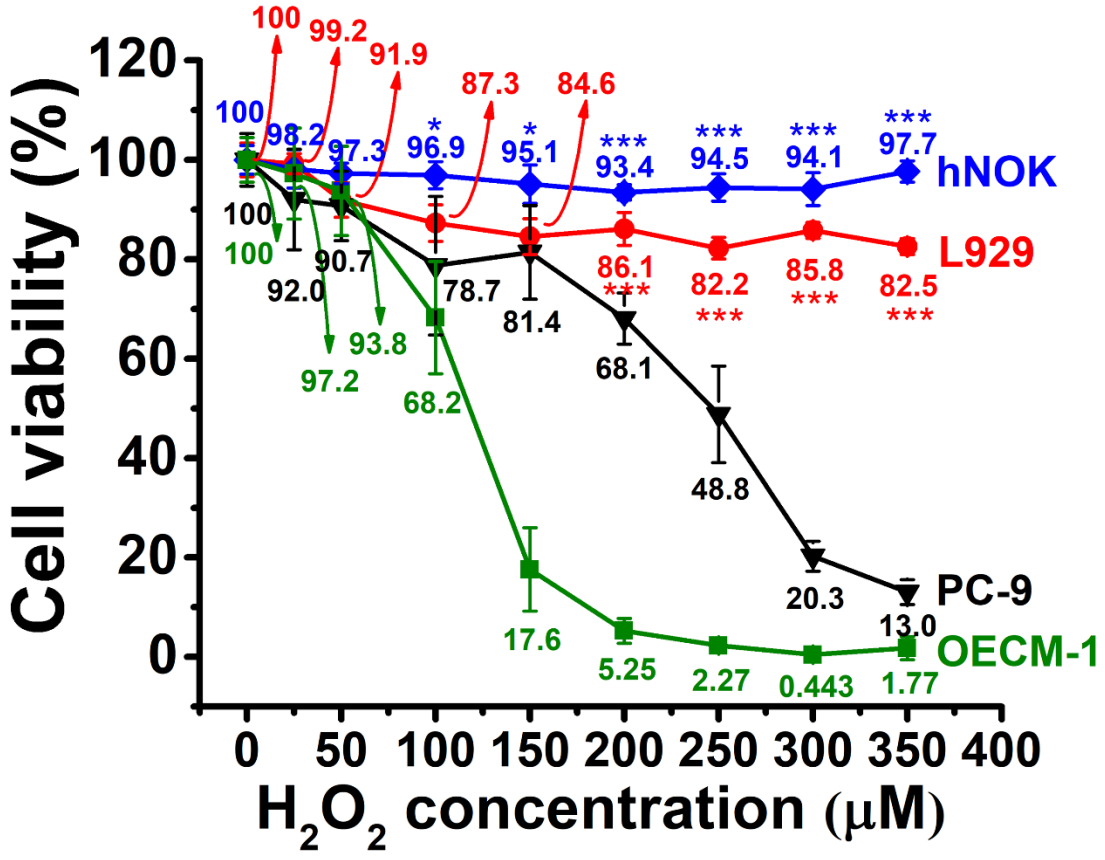

Fig. S7 Viabilities of the cancer (PC-9 and OECM-1) and normal (L929 and hNOK) cells after treatments with H_2O_2 of various dosages. Viability was analyzed using the MTT assay 72 h after the treatments. The plot presents the mean value of the data, whereas the error bars on each plot represent the standard error of the mean. The P values are indicated as *, **, and *** for $P < 0.05$, $P < 0.01$ and $P < 0.001$, respectively.

9. Population of viable cells in AnnV/PI-assay analysis

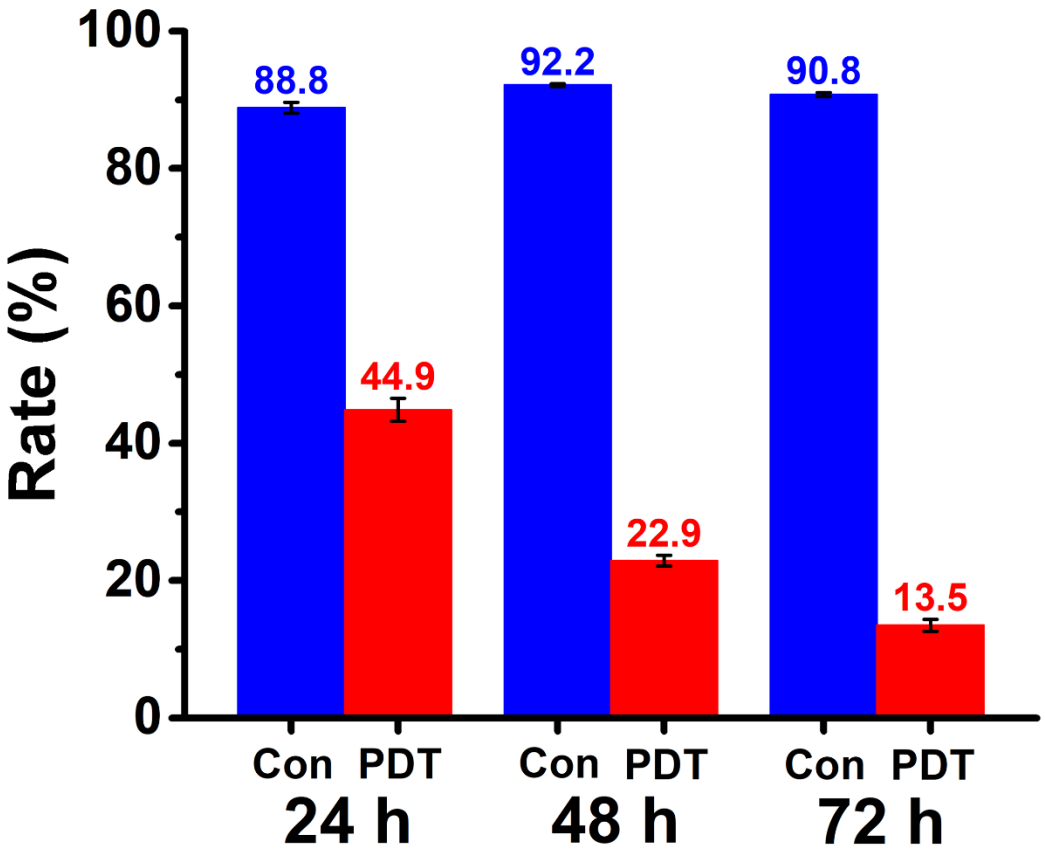

Fig. S8 Population variation of the viable cells (encompassed by quadrant [–,–]) with time according to the data of Fig. 4b, in which AnnV/PI assays were used for analysis. The plot presents the mean value of the data, whereas the error bars on each plot represent the standard error of the mean.

10. EPR for $^1O_2$ generation analysis

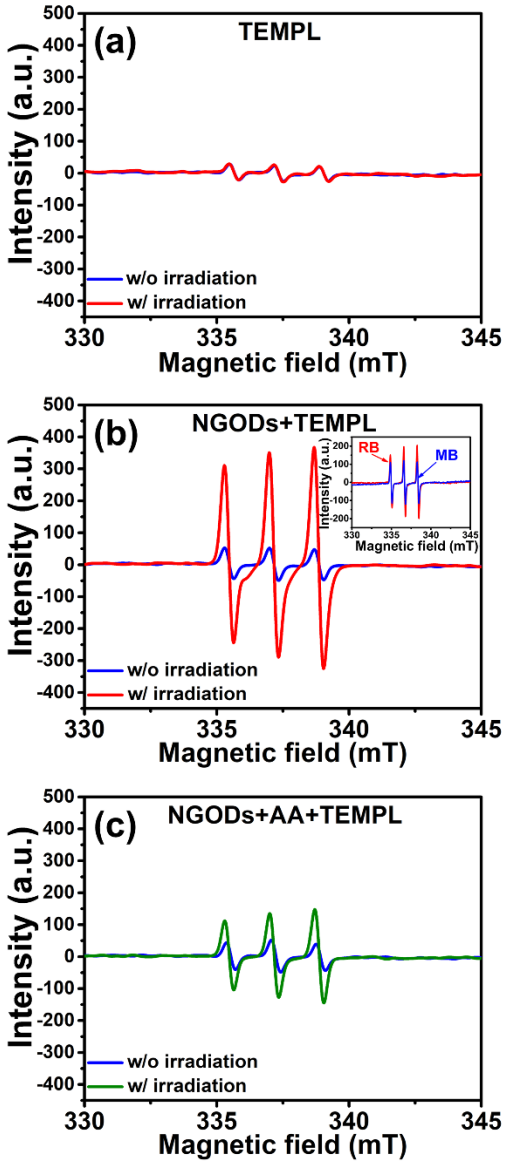

Fig. S9 EPR spectra of TEMPL solutions for $^1O_2$ generation analysis. (a) Nonirradiated and irradiated TEMPL solution. (b) Nonirradiated and irradiated NGOD–TEMPL solution. (c) Nonirradiated and irradiated NGOD–TEMPL–AA solution. The inset of panel (b) compares the spectra of the irradiated NGOD, RB, and MB solutions containing TEMPL. The concentrations of NGODs, RB, and MB were 10 μg mL^{-1}, that of AA was 0.1 mM, and that of TEMPL was 85 mM.

12. EPR for O_2^{-}•, HO_2•, and OH• generation analysis

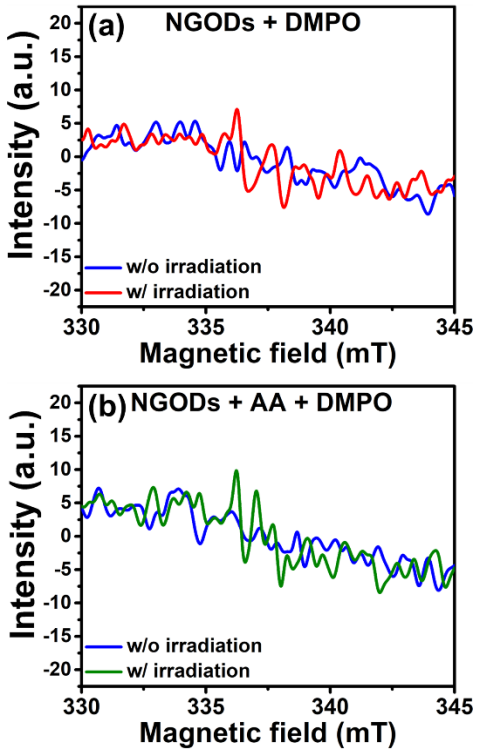

Fig. S10 EPR spectra of DMPO solutions for O_2^{-}•, HO_2•, and OH• generation analysis. (a) Nonirradiated and irradiated NGOD–DMPO solution. (b) Nonirradiated and irradiated NGOD–DMPO–AA solution. The concentrations of NGODs were 10 μg mL^{-1}, that of AA was 0.1 mM, and that of DMPO was 100 mM.

12. Amplex® Red method for H_2O_2 quantification

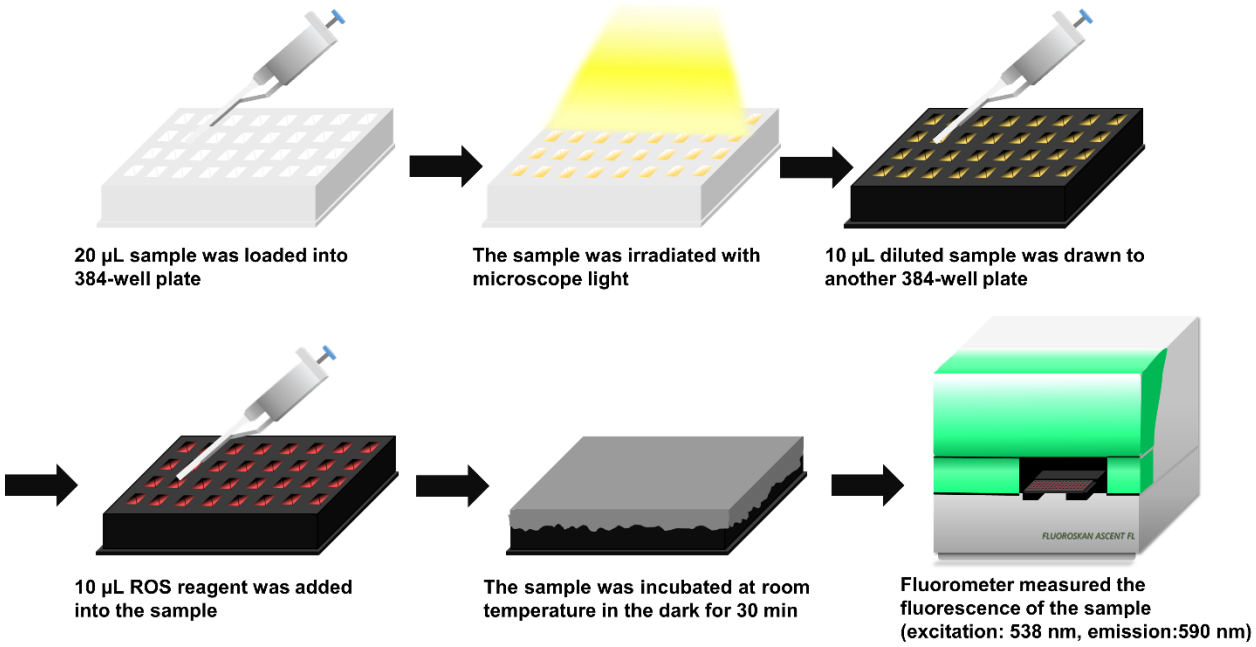

Fig. S11 Schematic of reaction process using Amplex® Red method to quantify the amount of produced H_2O_2.